ANTIOXIDANTS & REDOX SIGNALING
Volume 10, Number 10, 2008

DOI: 10.1089/ars.2007.1994

Original Research Communication

Redox Potential and the Response of Cardiac Ryanodine Receptors to CLIC-2, a Member of the Glutathione *S*-Transferase Structural Family

Chris Jalilian, Esther M. Gallant, Philip G. Board,[1] and Angela F. Dulhunty[1]

Abstract

The type 2 chloride intracellular channel, CLIC-2 , is a member of the glutathione *S*-transferase structural family and a suppressor of cardiac ryanodine receptor (RyR2) Ca^{2+} channels located in the membrane of the sarcoplasmic reticulum (SR). Modulators of RyR2 activity can alter cardiac contraction. Since both CLIC-2 and RyR2 are modified by redox reactions, we speculated that the action of CLIC-2 on RyR2 may depend on redox potential. We used a GSH:GSSG buffer system to produce mild changes in redox potential to influence redox sensors in RyR2 and CLIC-2. RyR2 activity was modified only when both luminal and cytoplasmic solutions contained the GSH:GSSG buffer and the effects were reversed by removing the buffer from one of the solutions. Channel activity increased with an oxidizing redox potential and decreased when the potential was more reducing. Addition of cytoplasmic CLIC-2 inhibited RyR2 with oxidizing redox potentials, but activated RyR2 under reducing conditions. The results suggested that both RyR2 and CLIC-2 contain redox sensors. Since cardiac ischemia involves a destructive Ca^{2+} overload that is partly due to oxidation-induced increase in RyR2 activity, we speculate that the properties of CLIC-2 place it in an ideal position to limit ischemia-induced cellular damage in cardiac muscle. *Antioxid. Redox Signal.* 10, 1675–1686.

Introduction

In striated muscle, Ca^{2+} mediates excitation–contraction (EC) coupling when action potential depolarization of the sarcolemma leads to activation of ryanodine receptor (RyR) Ca^{2+} release channels in the intracellular sarcoplasmic reticulum (SR) Ca^{2+} store. In cardiac muscle, the depolarization allows a Ca^{2+} influx through surface membrane L-type Ca^{2+} channels, and this Ca^{2+} activates the cardiac RyR (RyR2) by Ca^{2+}-induced Ca^{2+}-release (23). Modifications such as phosphorylation, nitrosylation, and redox reactions regulate RyR activity and allow the channel to respond to microenvironmental changes (15, 18, 21, 26, 29). GSH and GSSG are the major redox buffers in the cytosol and are present in healthy cells in concentrations that maintain a reduced cytoplasmic redox potential (~ -220 mV), and a more oxidized potential in the lumen of the SR (~ -180 mV) (27). Most studies of redox effects use addition of GSH or GSSG alone, creating extreme redox potentials which modify disulfide bridges involving protein cysteines (13, 14, 19, 22). Redox responses that are more physiologically relevant occur when "redox sensors" within the RyR detect milder changes in redox potential (16, 27). These responses do not depend on making or breaking disulfides and can be reversed by washout of redox buffers (16, 27). The responses have not been extensively studied, even though a quarter of the 80–100 cysteines in each RyR subunit (depending on the isoform) are available to sense redox potential (8). Physiological GSH:GSSG buffer systems applied to skeletal RyR (RyR1) channels do not alter channel activity when applied to only one side of the bilayer, but the channel becomes responsive to the redox potential when the buffer is applied to both sides (16, 27). In cardiac ischemia, regulatory thiols on RyR2 are influenced by oxidizing conditions, and the resulting Ca^{2+} release from the SR contributes to overload of cytosolic Ca^{2+} and necrosis (24). The effects on RyR2 activity of mild changes

Division of Molecular Bioscience, John Curtin School of Medical Research, Australian National University, ACT, Australia.
[1]Board and Dulhunty contributed equally to this work.

in redox potential that might occur during ischemia have not been examined.

RyR2 channels are regulated by members of the glutathione *S*-transferase (GST) structural family, GSTO1-1 (9), GSTM2-2 (1), and CLIC-2 (4, 11). The CLIC-2 (**c**h**l**oride **i**ntracellular **c**hannel type 2) protein belongs to the GST structural family (9), although it does not have *S*-thioltransferase activity (4) and it lacks the GSH binding site found in most GSTs (7). GSH present in the crystal structure of CLIC-2 does not covalently modify cysteine residues (7). Thus, CLIC-2 is not a conventional glutathione *S*-transferase enzyme, but it does respond to redox potential because its ability to form Cl^- channels is abolished by 5 m*M* DTT (7). The effect of CLIC-2 on RyR2 channels does not depend on disulfide formation because (a) it is reversed by CLIC-2 washout and by a CLIC-2 antibody, and (b) the effect of CLIC-2 is not altered by mutations of cysteine residues that could covalently modify the RyR2 protein complex (4, 11). It is suggested that an extended "foot loop" in the C-terminal domain of CLIC-2 may participate in a "foot-in-mouth" interaction with RyR2 (7). The effect of redox potential on the CLIC-2/RyR2 interaction has not been examined but is relevant because CLIC-2 may help reduce the effects of ischemic damage in cardiac myocytes by reducing RyR2 activity (4, 11).

Here we investigate the effect of redox potential on RyR2 activity and the regulatory action of CLIC-2. We find that CLIC-2 increases RyR2 activity under more reducing conditions, but decreases activity under more oxidizing conditions. These properties of CLIC-2 would allow it to limit cellular damage in the heart in times of oxidative stress.

Methods

Isolation of SR vesicles

Cardiac SR vesicles were prepared as previously described (13, 20).

Expression and purification of CLIC-2

CLIC-2 was expressed with an N-terminal poly-His tag and purified by Ni-agarose affinity chromatography as described in ref. 4. Recombinant CLIC-2 was purified by Ni-agarose immobilized metal affinity chromatography with modifications to the protocol outlined in ref. 32. The purity of the extract was assessed on Coomassie brilliant blue stained SDS–PAGE gels, and the apparent molecular weight was checked using a low molecular weight calibration kit (Amersham Pharmacia Biotech, Uppsala, Sweden). Multiple freezing (−70°C) and thawing resulted in a marked reduction in CLIC-2 activity so that small aliquots of freshly thawed material were used.

Regulation of redox potential

The redox potential was manipulated with a GSH:GSSG buffer (16). An oxidizing redox potential of −195 mV was established with either 2 m*M* GSH plus 0.5 m*M* GSSG or 0.2 m*M* GSH plus 0.05 m*M* GSSG (4:1 GSH:GSSG). A reducing redox potential of −220 mV was achieved with either 7.5 m*M* GSH plus 0.25 m*M* GSSG or 0.75 m*M* GSH plus 0.025 m*M* GSSG (30:1 GSH:GSSG). In single channel experiments, GSH and GSSG were freshly prepared and added individually in appropriate amounts to the *cis* and *trans* solutions. In Ca^{2+} release experiments, cardiac SR vesicles were equilibrated in freshly prepared GSH:GSSG solutions at 4°C for 30 min prior to commencing the experiment.

Single channel recording and analysis

Artificial lipid bilayers separating *cis* and *trans* solutions were formed (9, 13, 20). Single channel parameters were obtained using the Channel 2 program (developed by P.W. Gage and M. Smith, John Curtin School of Medical Research, Canberra, Australia). Experiments were carried out at 23 ± 2°C. Bilayer potential is expressed as the cytoplasmic relative to luminal and was changed every 30 s between +40 and −40 mV. Current was recorded continuously throughout the experiment at 5 kHz and was filtered at 1 kHz. The open probability (P_o) was measured using either a threshold discriminator (when one channel only opened) or from mean current, I' (when bilayers contained more than one active channel). For threshold detection, a threshold was set outside the noise at ~20% of the maximum open conductance. Currents exceeding the threshold were detected as channel openings. The mean current (I') is the average of all data points in a record. Relative I′ is approximately equal to relative P_o.

Ca^{2+} release from cardiac SR vesicles

A Cary 3 spectrophotometer was used to monitor extravesicular Ca^{2+} at 710 nm, using the Ca^{2+} indicator antipyrylazo III. Cardiac SR vesicles (100 μg/ml) were added to a solution containing 100 m*M* KH_2PO_4, 0.4 m*M* antipyrylazo III, 1 m*M* Na_2ATP, and 4 m*M* $MgCl_2$, controlled at a temperature of 25°C and magnetically stirred (10). The protocol is shown in Fig. 6 and described in the figure legend. A calibration curve of optical density changes with four additions of 12.5 μM $CaCl_2$ was constructed. The calibration curve was not altered by the presence of CLIC-2, caffeine, or ruthenium red. Ca^{2+} release (the rate of caffeine induced Ca^{2+} release minus the rate with thapsigargin) was used calculated as nmoles of Ca^{2+} per mg of SR vesicles per min (5).

Statistics

Average data are presented as mean ± SEM. The significance of differences between control and test values were tested using a Student's *t* test for paired data or a sign test (25), as appropriate. A p value of <0.05 was considered significant.

Results

Cardiac RyR2 channels in bilayers

Effects of changing redox potential on RyR2 channel activity and the response to CLIC-2. Channels were recorded with a cytoplasmic [Ca^{2+}] of 10 μM and luminal [Ca^{2+}] of 1 m*M*. The 4:1 GSH/GSSG buffer was added to the *cis* and *trans* solutions to produce a symmetrical oxidising redox potential of -195mV (16). As for RyR1 (16), adding the redox buffer to either *trans* (n = 3, Fig. 1A) or *cis* (n = 5, Fig. 1B) solution alone did not alter RyR2 activity, but the channels were strongly activated when 4:1 GSH:GSSG was added to both sides of the bilayer (Fig. 1C, panel 2). This activation was rapidly reversed by perfusing the GSH:GSSG buffer from one side of the bilayer (Fig. 1C, panel 3).

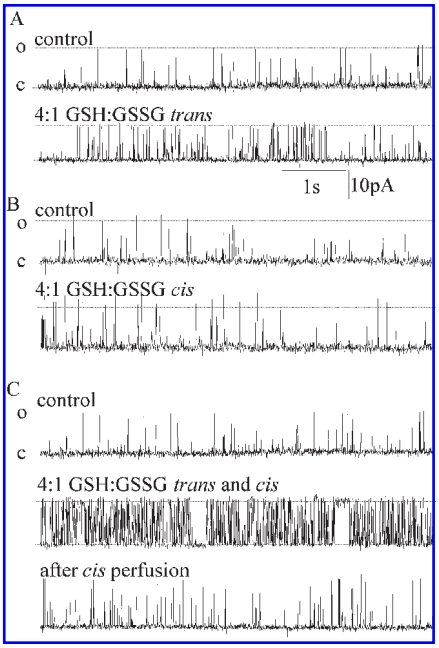

FIG. 1. RyR2 channel responses to oxidizing redox potentials (2.0 m*M* GSH: 0.5 m*M* GSSG) on one or both sides of the bilayer. Records show 6 s of RyR2 channel activity recorded at +40 mV, with channel opening upward. (**A**) Before (*upper panel*) and after (*lower panel*) addition of 4:1 GSH:GSSG to the *trans* solution. (**B**) Before (*upper panel*) and after (*lower panel*) addition of 4:1 GSH:GSSG to the *cis* solution. (**C**) Before (*upper panel*) and after (*central panel*) addition of 4:1 GSH:GSSG to the *cis* and *trans* solutions and after removal of the buffer from the *cis* solution (*lower panel).* In this and subsequent figures, channel opening is shown from the closed level (C) to a maximum open level (O).

Oxidizing redox potential. The increase in activity with a symmetrical oxidizing buffer was seen using either 2.0:0.5 m*M* GSH:GSSG in Figs. 1B and 2A, or 0.2:0.05 m*M* GSH:GSSG in Fig. 2D in 11 of 11 experiments. Channel parameters were determined by threshold analysis in experiments with 2.0:0.5 m*M* GSH:GSSG (Figs. 2A–C). Since the open probability of the RyR2 channels showed the usual scatter of values (0.01 to 0.35), relative changes were used to assess the effects of redox potential and of CLIC-2. There was a 6.3 ± 1.30-fold increase in average relative open probability (P_o, Fig. 2B). The absolute P_o was 0.067 ± 0.07 before adding 4:1 GSH/GSSG and 0.17 ± 0.082 after adding GSH/GSSG. The increase in open probability was due to a significant 1.6 ± 0.19-fold increase in mean open time (T_o) from a control value of 2.25 ± 0.27 ms. There was a corresponding significant fall in the mean closed time (T_c) to 0.33 ± 0.08 of its control value of 134 ± 28 ms. More than one channel opened in three of four experiments with 0.2:0.05 m*M* GSH:GSSG (Fig. 2D and E), thus relative P_o was determined from mean current (see Methods) and open and closed times not measured. However, the records show longer openings under the oxidizing conditions and briefer closures (Fig. 2D).

CLIC-2 added to the cytoplasmic (*cis*) solution with symmetrical oxidizing redox potentials produced a marked reduction in channel activity (panel 3 in Fig. 2A and D). CLIC-2 at 4 μM produces maximal inhibition of RyR2 channels (11) and this concentration was used in all experiments. Relative P_o fell (Fig. 2C) to 0.42 ± 0.06 of the value in 4:1 GSH:GSSG (2.0:0.5 m*M*) before addition of CLIC-2. P_o was 0.16 ± 0.04 before, and 0.06 ± 0.01 after CLIC-2 addition. The fall in activity was due to a ~3-fold increase in the mean closed time (T_c) (Fig. 1B and C). There was no significant change in mean open time (T_o) (Fig. 1B and C). Similarly, the relative P_o with 0.2:0.05 m*M* GSH:GSSG fell by ~50% after addition of 4 m*M* CLIC-2 (Fig. 2E). Similar changes in gating were seen when the redox potential was unregulated (4, 11).

In addition, results in Fig. 2 show firstly that the ratio of GSH:GSSG rather than the GSH or GSSG concentrations determine the response of the RyR. Secondly, the effects of the oxidizing redox potential and CLIC-2 are reversed by perfusion of the *cis* chamber (Fig. 2E and F) as are the individual effects of the oxidizing buffer and CLIC-2 (4, 11, 16). Finally, similar results were obtained with analyses of 1 min (Fig. 2B and C) or 4 min (Fig. 2E and F), suggesting that the results were not distorted in the shorter analysis. In four control experiments, addition of CLIC-2 to the *trans* chamber with symmetrical 3:1 GSH/GSSG did not change channel activity.

More reducing redox potential. In contrast to the RyR2 activation with oxidizing redox potentials, there was a fall in channel activity with reducing redox potentials, using either 7.5:0.25 m*M* GSH:GSSG (Figs. 3A–C), or 0.75:0.025 m*M* GSH:GSSG (Figs. 3D and E). There was a significant fall in average relative open probability to 0.23 ± 0.16% of control in the seven experiments with 7.5:0.25 m*M* GSH:GSSG (Fig. 3B). The open probability was 0.065 ± 0.033 before and 0.005 ± 0.003 after addition of 30:1 GSH:GSSG. There was a significant decrease in open time and increase in closed time. Channels exposed to 30:1 GSH:GSSG (*cis* and *trans*) using lower concentrations of 0.75:0.025 m*M* GSH:GSSG were also inhibited by the reducing buffer (Fig. 3D). Relative P_o was determined from mean current because the bilayer contained two channels in six of seven experiments. The average relative P_o fell to ~50% after exposure to the reducing buffer (Fig. 3E).

In contrast to inhibition by CLIC-2 with the oxidizing redox potential (above), adding 4 μM CLIC-2 to the cytoplasmic side of the RyR2 channels with the reducing redox potential increased channel activity (Fig. 3A and D, 3rd panel). Average relative P_o from seven experiments with 7.5:0.25 m*M* GSH:GSSG increased 4.1 ± 1.5-fold (Fig. 3B). The absolute P_o was 0.005 ± 0.003 before and 0.028 ± 0.011 after adding CLIC-2, with significant increases in the mean open times and reductions in the mean closed time (Fig. 3B and C). Similarly, with 0.75:0.025 m*M* GSH:GSSG in the *cis* and *trans* solutions, the relative P_o (analyzed over a 4 min continuous recording) increased 2.5-fold after addition of 4 m*M* CLIC-2 (Fig. 3E). Therefore, the GSH:GSSG ratio rather than buffer concentration again determined the response to CLIC-2. The increase in P_o with addition of CLIC-2 was reversed when the *cis* chamber was perfused and the effects of CLIC-2 were similar with analyses over 1 min (Fig. 3B and C) or 4 min (Fig. 3E).

Effects of ATP on the RyR2 response to redox potential and CLIC-2. ATP (2 m*M*) was added before 30:1 GSH:GSSG

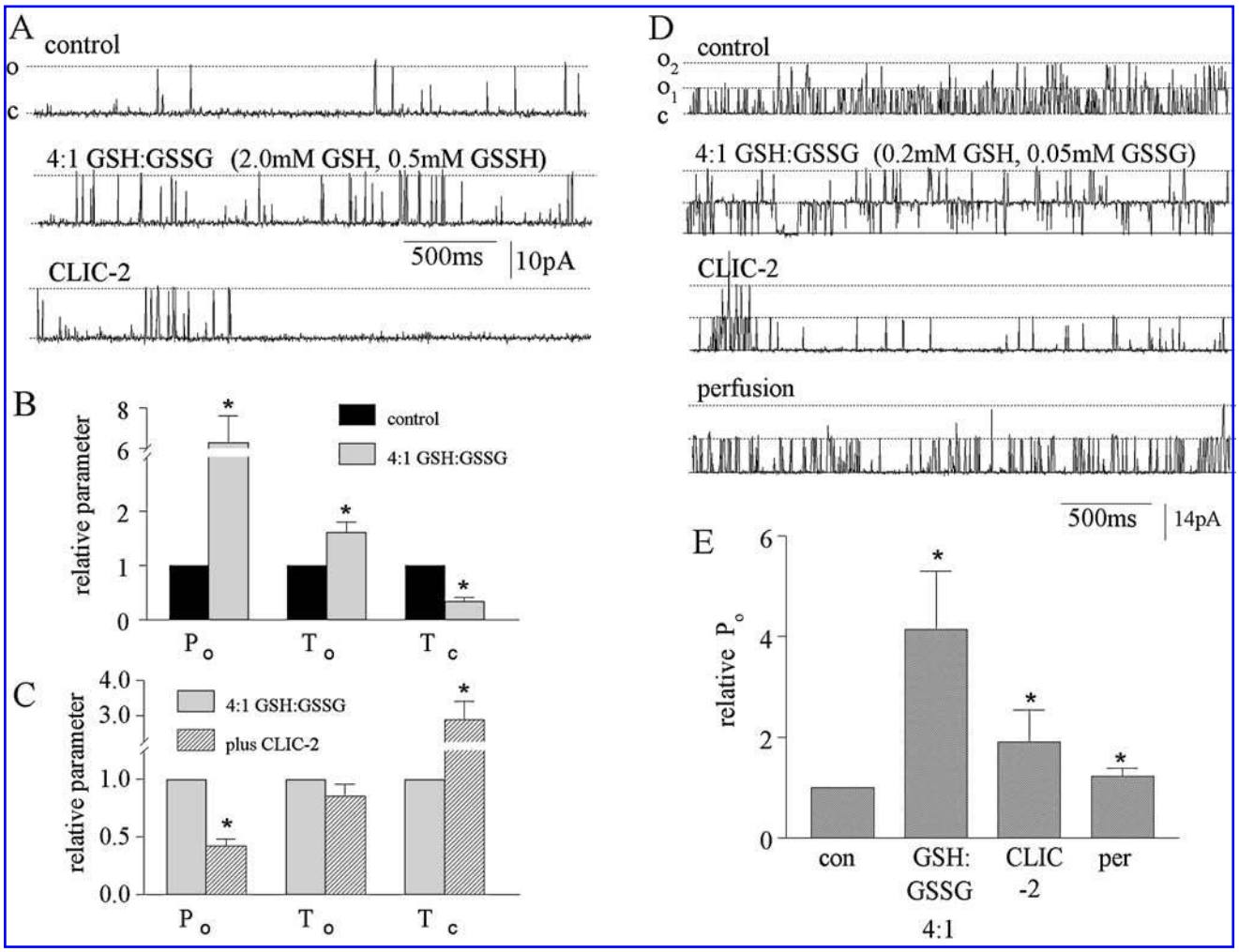

FIG. 2. RyR2 channel activation by the oxidizing 4:1 GSH:GSSG buffer in the *cis* and *trans* solutions and inhibition by 4 μM CLIC-2. (**A**)–(**C**) Data obtained using 2.0 m*M* GSH and 0.5 m*M* GSSG. (**A**) A single RyR2 channel recorded at +40 mV, opening upward. The records show 3 s of channel activity before (*upper panel*) and after (*central panel*) addition of 4:1 GSH:GSSG buffer and the subsequent addition of CLIC-2 (*lower panel*). (**B** and **C**) The average results of analysis of seven experiments. Relative values are shown for open probability (P_o), mean open time (T_o), and mean closed time (T_c). (**B**) Average data after addition of 4:1 GSH:GSSG (*gray bins*), relative to activity before addition of buffer (*black bins*). (**C**) Average values in the presence of CLIC-2 (*hatched bins*) relative to values before addition of CLIC-2 (*gray bins*). (**D**) and (**E**) Data with 0.2 m*M* GSH and 0.05 m*M* GSSG. (**D**) Current records from a bilayer containing two active channels which opened individually to O_1 and together to O_2. Channel opening increased after symmetrical addition of GSH:GSSG (*panel 2*), fell after *cis* addition of CLIC-2 (*panel 3*), and returned to control after perfusion of GSH:GSSG and CLIC-2 from the *cis* chamber (*panel 4*). (**E**) Average relative open probability from four experiments, determined from mean current during eight consecutive 30 s periods under each condition, relative to mean current over the same period under control conditions. In this and subsequent channel figures, relative values were calculated for individual experiments and the average of relative values obtained. *Asterisks* indicate significant differences from the preceding condition.

in seven experiments. The relative open probability increased with ATP (Fig. 4A) to 3.5 ± 1.0-fold above control (Fig. 4B). When 30:1 GSH:GSSG was added there was an **increase** in activity (Fig. 4A, panel 3), in contrast to the decrease in the absence of ATP (Fig. 3). The relative P_o increased significantly above that with ATP alone and was 6.3 ± 2.0-fold greater than control (Fig. 3B). Addition of CLIC-2 caused a further significant increase in relative P_o to an average value that was 12.9 ± 4.7-fold greater than the unregulated control value, or 2.2 ± 0.55-fold greater than before CLIC-2 addition.

CLIC-2 stabilizes subconductance activity in channels whose overall activity was depressed by CLIC-2 (4). This enhanced subconductance activity was seen in channels activated by CLIC-2 under reducing redox conditions and was particularly apparent in channels that were super-activated by ATP and CLIC-2. A prolonged substate at a level that was ~1.67 times the single channel conductance can be seen in the fourth panel in Fig. 4A. The record in Fig. 4C shows two open levels O1 and O2 (with relative conductances of 1.0 and 2.0 times the full single channel conductance). Maintained openings are apparent at levels of 0.33, 0.67, 1.0, 1.33, 1.67, and 2.0 in the records and in the all-points histogram in Fig. 3D. The equally spaced levels indicate that both channels were opening to subconductance levels that were ~33% and ~67% of their maximum conductance.

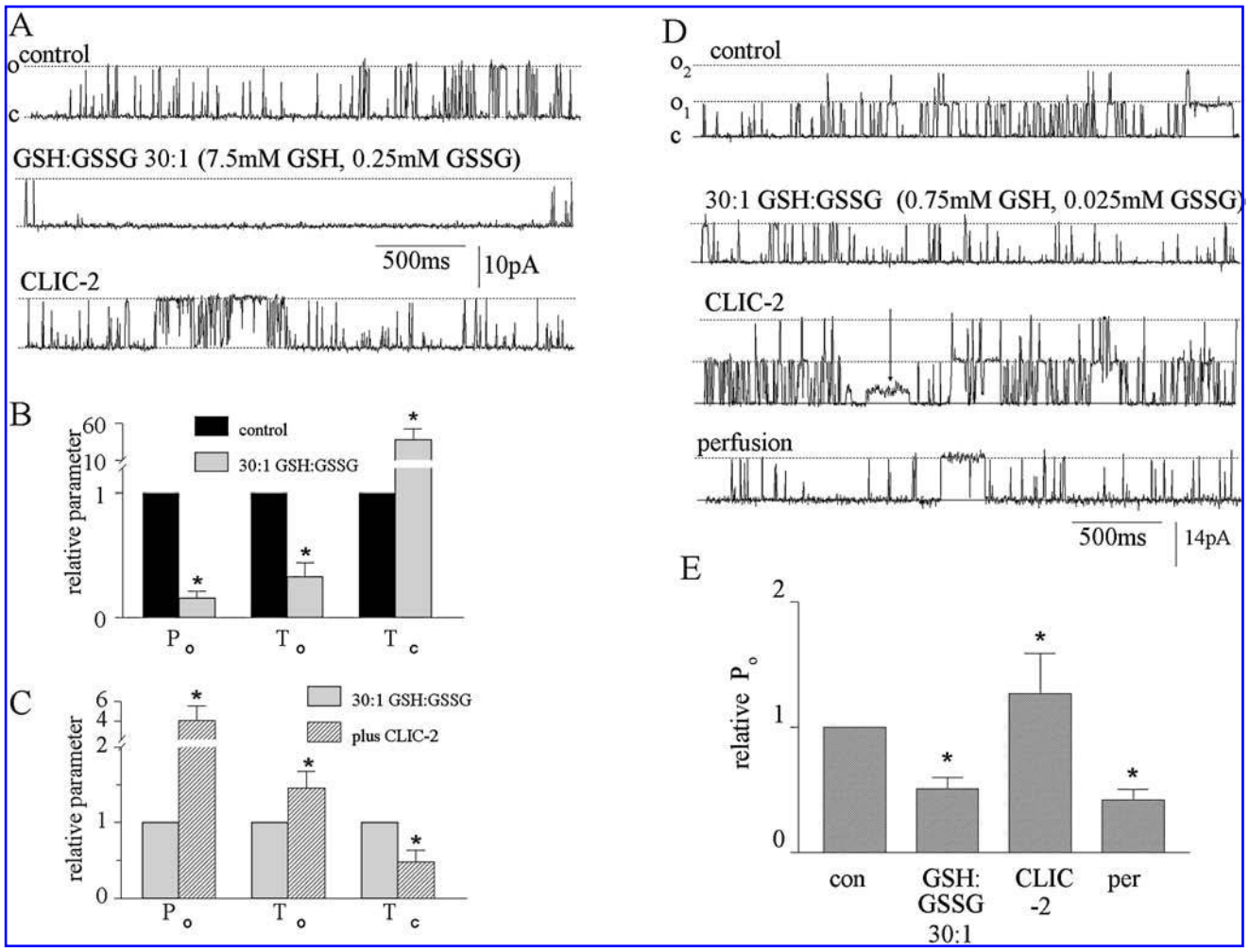

FIG. 3. RyR2 channel inhibition by addition of the reducing 30:1 GSH:GSSG buffer to the *cis* and *trans* solutions and activation by addition of 4 μM CLIC-2. (**A**)–(**C**) data with 7.5 m*M* GSH and 0.25 m*M* GSSG. (**A**) A single RyR2 current recorded at +40 mV, with channel opening upward. The records show 3 s of activity before (*upper panel*) and after (*central panel*) addition of 30:1 GSH:GSSG and subsequent addition of CLIC-2 (*lower panel*). (**B** and **C**) show relative parameter values for open probability (P_o), mean open time (T_o), and mean closed time (T_c) for seven experiments. (**B**) Average data after addition of 4:1 GSH:GSSG (*gray bin*) relative to values before addition of 4:1 GSH:GSSG (*black bins*). (**C**) Average values in the presence of CLIC-2 (*hatched bins*) relative to values measured before addition of CLIC-2 (*gray bins*). (**D** and **E**) Data with 0.75 m*M* GSH and 0.025 m*M* GSSG. (**D**) Current records from a bilayer containing two active channels which opened individually to O_1 and together to O_2. Channel opening decreased after the symmetrical addition of GSH:GSSG (*panel 2*), increased after *cis* addition of CLIC-2 (*panel 3*), and returned to control after perfusion of GSG:GSSG and CLIC-2 from the *cis* chamber (*panel 4*). Note the long CLIC-2 induced subconductance opening (*vertical arrow*) after the addition of CLIC-2. (**E**) Average relative open probability from six bilayers determined from the mean current during eight consecutive 30 s periods under each condition relative to mean current over the same period under the initial control conditions.

The influence of ATP on the response of RyR2 to oxidizing conditions (Fig. 4E and F) was similar to that in its absence (Figs. 1 and 2). Addition of 4:1 GSH:GSSG produced at 1.5-fold increase in the activity of RyR2 that had previously been activated 3.6-fold by ATP (Fig. 4E and F). Addition of CLIC-2 produced a ~20% decline in activity, which was less than seen without ATP. Channel activity returned to control levels when the *cis* chamber was perfused to remove ATP, GSH:GSSG, and CLIC-2, indicating that the effects of each compound was reversible.

Effects of asymmetrical redox potentials RyR2 and its response to CLIC-2. In healthy cells, the redox potential in the cytoplasm is reducing, whereas that in the SR lumen is oxidizing. To approximate this situation, we added 30:1 GSG:GSSG (7.5:0.25 m*M*) to the *cis* solution and 4:1 GSG:GSSG (2:0.5 m*M*) to the *trans* solution, and then 4 μM CLIC-2 to the *cis* solution. Channel activity increased with the addition of the redox buffers (Fig. 5A). The ~3-fold increase in relative P_o was significant (Fig. 5B) but was significantly less than the ~6-fold increase with 4:1 GSG:GSSG on both sides of the bilayer (Fig. 2). There was no consistent change in activity with CLIC-2 under these conditions (Fig. 5B). Therefore, the action of CLIC-2 depends on the combined effect of the redox potential (GSH:GSSG ratio) in the *cis* and *trans* chamber.

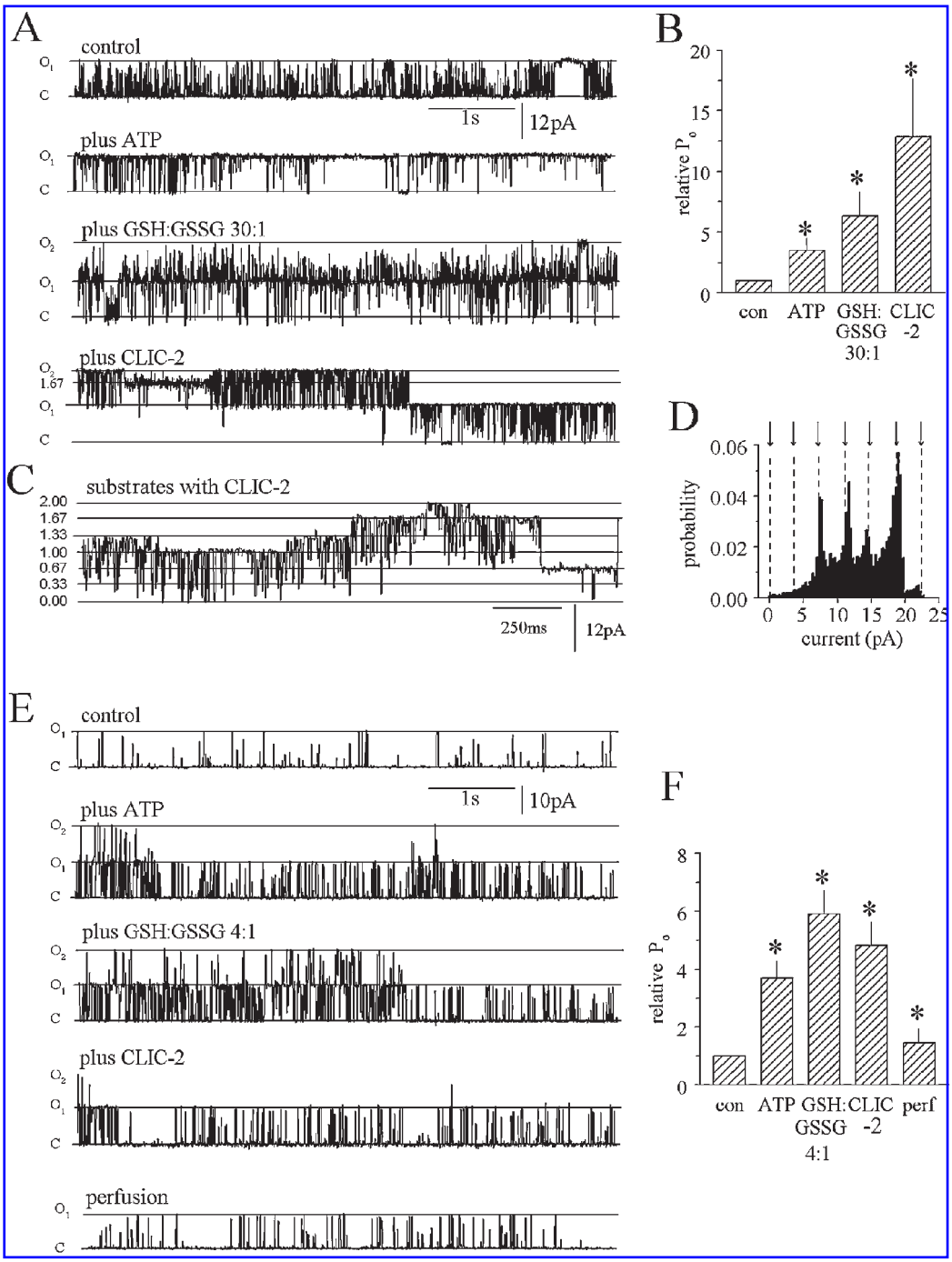

FIG. 4. In the presence of ATP, RyR2 channels are activated by the addition of either the reducing 30:1 GSH:GSSG (7.5:0.25 m*M*) buffer or oxidizing 4:1 GSH:GSSG (2.0:0.5 m*M*) to the *cis* and *trans* solutions. Channels were then either further activated by addition of 4 μM CLIC-2 under reducing conditions or inhibited by CLIC-2 under oxidising conditions. (**A–D**) Adding 30:1 GSH:GSSG and CLIC-2 in the presence of ATP. (**A**) Currents from a bilayer containing two RyR2 channel recorded at +40 mV, with channel opening to a maximum open level for one channel (O_1) or to O_2 when both channel open simultaneously ($O_2 = 2xO_1$**)**. The records show 6 s of activity before (*upper panel*) and after (*second panel*) addition of 2 m*M* ATP, then 30:1 GSH:GSSG buffer (*third panel*) and then CLIC-2 (*lower panel*) where a substate level at 1.67 O_1 is maintained for more than 1 s (*dotted line*). (**B**) Average relative open probability (P_o, seven experiments) under control conditions at the start of the experiment (*bin 1*), after adding ATP (*bin 2*), 30:1 GSH:GSSG (*bin 3*), and CLIC-2 (*bin 4*). Relative open probability is the mean current under each condition relative to mean current before exposure to ATP, measured over two consecutive 30 s periods. (**C**) A 2 s recording from a bilayer with two channels opening. The current dwelt at each of 6 levels for several seconds. The full conductance level for one channel opening is represented by a value of 1.0, a level of 2.0 is reached when the two channels open simultaneously to their maximum conductances. Each level is a multiple of 0.33 of the maximum single channel conductance. (**D**) All points histogram from the current in (**C**), each of the six open levels forms a peak in the histogram (*arrows*). (**E** and **F**) Adding 30:1 GSH:GSSG and CLIC-2 in the presence of ATP. (**E**) Currents from a bilayer with two RyR2 channels opening at +40 mV, 6 s of channel activity are shown before (*upper panel*) and after (*second panel*) addition of 2 m*M* ATP, then 4:1 GSH:GSSG buffer (*third panel*), and CLIC-2 (*fourth panel*), then channel activity after perfusion of ATP, GSH:GSSG, and CLIC-2 from the *cis* chamber only (*fifth panel*). (**F**) Average relative open probability (P_o, five experiments, determined from mean current) at the start of the experiment (*bin 1*), after adding ATP (*bin 2*), 4:1 GSH:GSSG (*bin 3*), and finally CLIC-2 (*bin 4*). Open probability is expressed relative to the initial control open probability before exposure to ATP and was measured over eight consecutive 30 s periods under each condition.

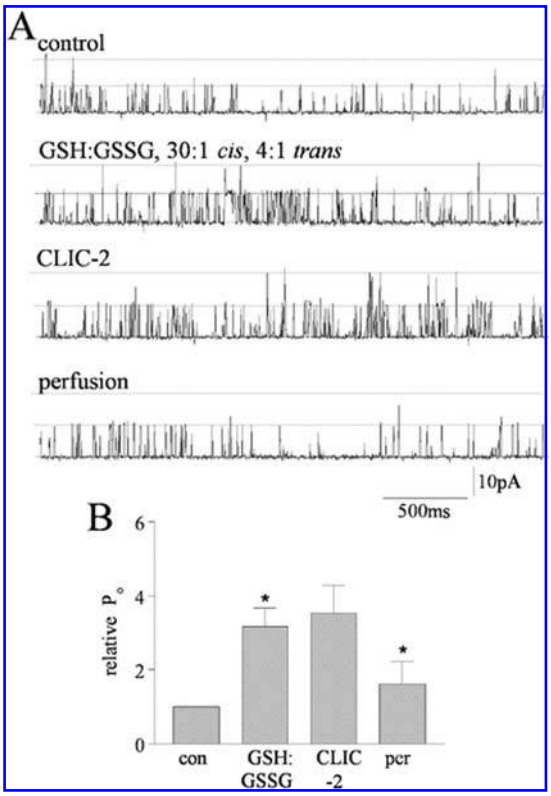

FIG. 5. Effects of CLIC-2 on RyR2 with a reducing cytoplasmic (*cis*) redox buffer (30:1 GSH:GSSG, 7.5:0.25 m*M*) and oxidizing luminal (*trans*) buffer (4:1 GSH:GSSG, 2.0:0.5 m*M*). (**A**) Currents from a bilayer containing two RyR2 channels recorded at +40 mV, with channel opening upward a maximum open level for one channel (O_1) or to O_2 when both channels open simultaneously ($O_2 = 2xO_1$); 3 s of channel activity is shown before (*upper panel*) and after adding the appropriate GSH:GSSG buffer to the *cis* and *trans* chamber (*second panel*), and then *cis* CLIC-2 (*third panel*). The *final panel* shows channel activity after perfusion of ATP, GSH:GSSG, and CLIC-2 from the *cis* chamber. (**B**) Average relative P_o (from 10 experiments, determined from mean current) at the start of the experiment (*bin 1*), after adding GSH:GSSG (*bin 2*), and then CLIC-2 (*bin 3*), and after perfusion of the *cis* chamber (*bin 4*). Open probability is expressed relative to the initial control open probability before exposure to redox buffer and was measured over eight consecutive 30 s periods.

Ca^{2+} release from cardiac SR

Ca^{2+} release from SR vesicles reveals the response of the RyR in a more intact situation than the lipid bilayer, although the population response that does not reveal the kinetics of individual channels. The technique is most powerful when used in conjunction with single channel experiments (4, 10). The response of Ca^{2+} release to the GSH:GSSG buffer system and the response to CLIC-2 under these redox conditions have not been examined previously. The experiments were done to test the hypothesis that the RyR in intact vesicles would respond to redox potential and CLIC-2 in the same way as the RyR in the isolated bilayer situation.

Caffeine was used to stimulate Ca^{2+} release using the protocol shown in Fig. 6. The rate of caffeine-induced release fell from 64.9 ± 10.0 to 39.3 ± 2.03 n*M*/mg/min with CLIC-2 (n = 8) (Fig. 7A and D) in the absence of redox buffers, as previously seen with Ca^{2+}-induced Ca^{2+} release (4). To allow GSH:GSSG equilibration in the lumen of the SR (16), vesicles were exposed to GSH:GSSG solutions for 30 min before commencing the experiment. Curiously, exposure to the oxidizing redox buffer did not alter the rate of caffeine-induced Ca^{2+} release (n = 8–9, Fig. 7). In contrast, the reducing redox buffer produced a 38.2% decrease in the rate of caffeine-induced Ca^{2+} release to 45.4 ± 5.3 n*M*/mg/min from a control rate of 64.9 ± 10.0 n*M*/mg/min (n = 8–9). Addition of 4 μM CLIC-2 with the oxidizing redox potential resulted in a significant decrease (Fig. 7B and D) from 70.2 ± 11.7 to 41.2 ± 6.4 n*M*/mg/min (n = 8–9). When the redox potential was reducing (Figs. 7C and D), CLIC-2 caused a 52% increase in Ca^{2+} release from 45.5 ± 5.4 to 69.0 ± 9.0 n*M*/mg/min (n = 8–10). Therefore, the effects of reducing redox potential and of CLIC-2 were similar in SR vesicle and single channel situations.

Discussion

The novel results show that the activity of the cardiac RyR2 channels is dependent on a regulated redox potential on either side of the SR membrane. Channel activity is enhanced if both the cytoplasmic and luminal solutions are clamped to a more oxidizing redox potential, but depressed if both solutions are clamped to a more reducing redox potential. The dynamic ability of CLIC-2 to regulate RyR2 in a manner that depends on redox potential is demonstrated. This is the first report of an endogenous regulator of the RyR2 that can either decrease or increase channel activity depending on a redox potential.

In vivo redox potentials and redox buffer concentrations

The total *in vivo* concentration of GSH and GSSG is 1–5 m*M*. GSSG concentrations of 0.05 m*M* in the cytoplasm and 0.3 m*M* in ER lumen have been measured (2). In this study we generally used higher concentrations of GSH and GSSG so that the buffers quickly equilibrated with the solution bathing the RyR channel. This did not alter the responses of RyR2, as similar effects were seen with lower concentrations, indicating that the GSH:GSSG ratio rather than the absolute concentrations was important and showing that the "mildness" of the redox conditions depended on the presence of both oxidizing and reducing reagents, rather than their concentrations.

Effects of redox potential on RyR2 channels and caffeine-induced Ca^{2+} release from SR

The activity of RyR2 channels in bilayers fell with reducing redox potentials and increased with oxidizing potentials as with for RyR1 channels (16). Ca^{2+} release from SR vesicles under reducing conditions mimicked the channel response, but unexpectedly, the oxidizing redox potential did not alter Ca^{2+} release. This was likely due to the luminal [GSSH] in the vesicle experiments being set by the glutathione transporter that selects GSH in preference to GSSG and transports GSSG slowly (2, 16). Therefore, the GSH:GSSG in the lumen may have been higher than in the extravesicular solution (and transiently reducing). The unaffected release under this condition is consistent with the

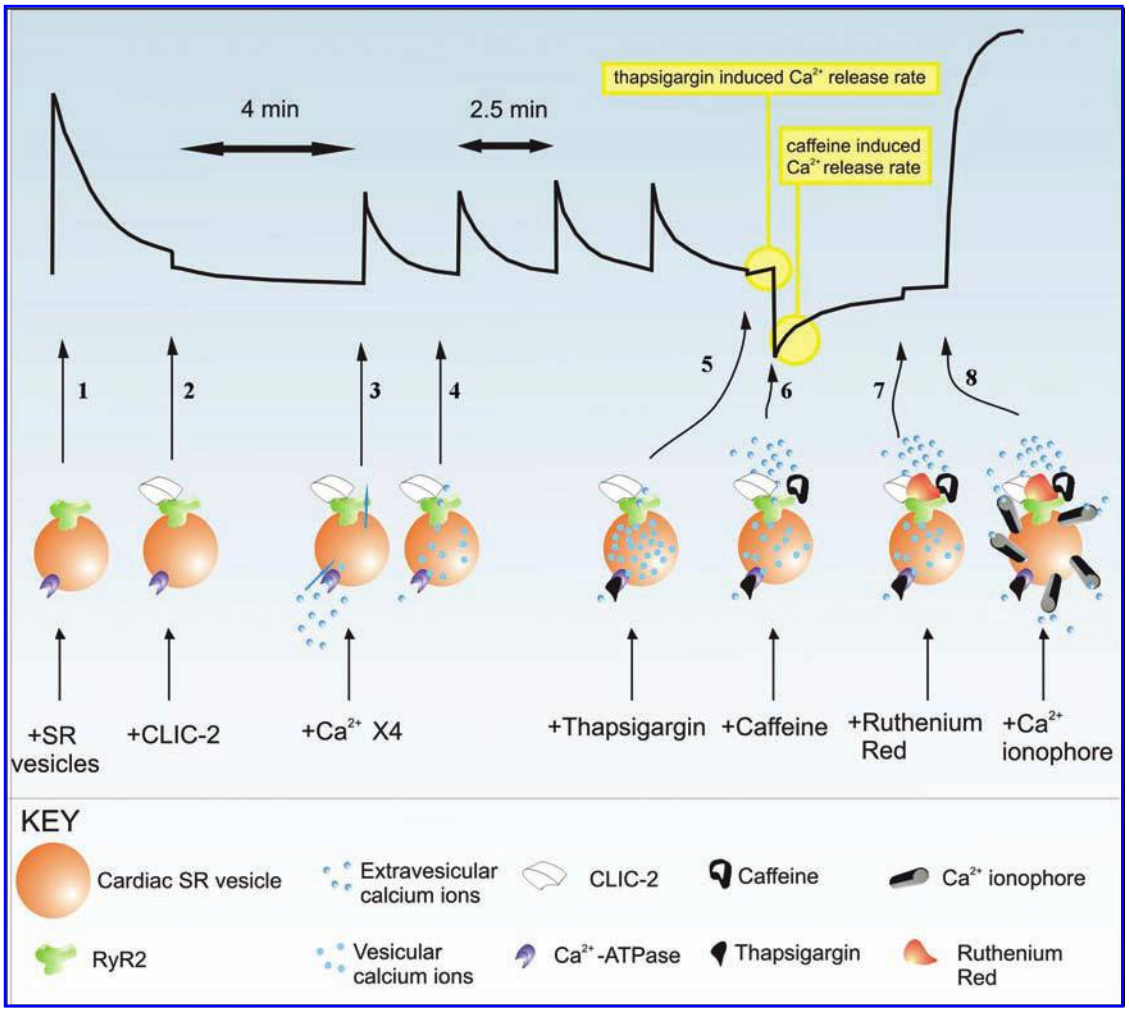

FIG. 6. A typical Ca^{2+} release experiment (with CLIC-2) showing a record of optical density as a function of time. Extravesicular Ca^{2+} was measured with the Ca^{2+} indicator antipyrylazo III at 710 nm. Cardiac SR vesicles were added to the cuvette (*arrow 1*). The increase in $[Ca^{2+}]$ with the initial vesicle addition was taken up as the Ca^{2+} ATPase was activated by MgATP. CLIC-2 (4 μM) was added (*arrow 2*) and equilibrated for 4 min. The SR was then loaded with four additions of 7.5 μM Ca^{2+} (30 μM total) (the first two additions indicated by *arrows 3* and *4*). Thapsigargin (2.25 μM) was added (*arrow 5*) to block the Ca^{2+}-ATPase, and then caffeine (4 or 5 m*M*) (*arrow 6*). Caffeine immediately reduced OD, which then an increase as caffeine stimulated Ca^{2+} release. Ruthenium red was added (*arrow 7*) and then Ca^{2+} ionophore (*arrow 8*). Block of Ca^{2+} release with ruthenium red verified that caffeine-induced Ca^{2+} release was through RyR2. Ca^{2+} release with the ionophore indicated that Ca^{2+} remained in the vesicles once the RyR2-releasable store had been depleted by caffeine. (For interpretation of the references to color in this figure legend, the reader is referred to the web version of this article at www.liebertonline.com/ars).

fact that channel activity is lower and closer to unregulated levels if the redox potential is oxidizing on one side of the membrane and reducing on the other (Fig. 5) (16). The decrease in Ca^{2+} release with an extravesicular reducing redox potential is consistent with effects of symmetrical reducing conditions on channel activity and indicates that the higher GSH:GSSG ratio was maintained in the lumen by the more efficient GSH transport.

Effects of redox potential on the response of RyR2 to CLIC-2.

The oxidizing redox potential was accompanied by a CLIC-2-dependent depression of RyR2 activity and Ca^{2+} release, whereas enhanced activity was seen with reducing redox potentials. This reversal could be due to the effect of redox potential on either RyR2 or on CLIC-2. At least part of the difference can be attributed to CLIC-2 itself because ATP reversed the inhibitory effect of the reducing redox potential on RyR2, yet the action of CLIC-2 on RyR2 channels was unaltered. Any of several free -SH groups seen in the crystal structure of CLIC-2 could sense redox potential (7). The response of the RyR2 to CLIC-2 was not simply a function of initial channel activity. CLIC-2 inhibited low activity channels (in the absence of activating ligands) or channels activated by Ca^{2+} or ATP, and prevents channel activation by Ca^{2+} or ATP (11). Figure 5 shows that RyR mildly activated with asymmetrical GSH:GSSG ratios were not inhibited by CLIC-2. Conversely, channels activated by ATP under reducing conditions were further activated by CLIC-2 (Fig. 4).

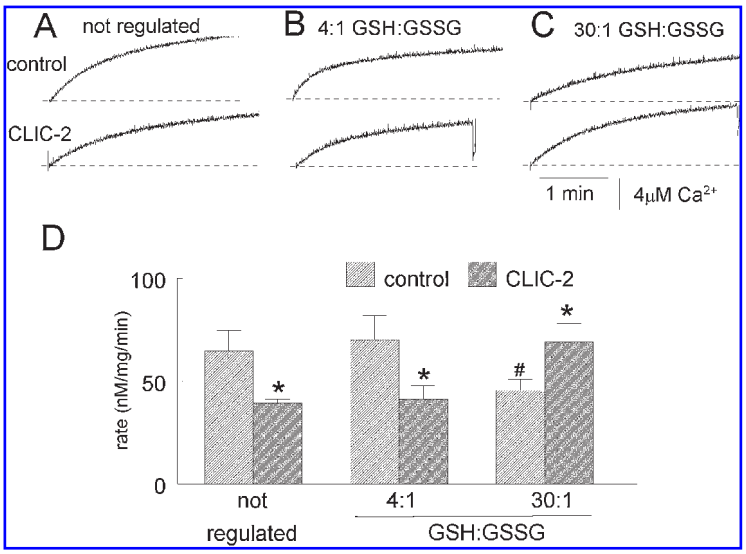

FIG. 7. Effect of 30 min exposure GSH:GSSG buffers on Ca^{2+} release and effects of 4 μM CLIC-2. (**A–C**) Spectrophotometer recordings of Ca^{2+} release as a function of time after caffeine addition under conditions (*upper panel*) and after exposure to CLIC-2 (*lower panel*). (**A**) Redox potential unregulated; (**B**) oxidizing with 4:1 GSH:GSSG; (**C**) reducing with 30:1 GSH:GSSG; (**D**) average rates of caffeine-induced Ca^{2+} release in nM/mg/min (six experiments) in the absence (control, *wide stippled bin*) and presence (*narrow stippled bin*) of CLIC-2, in solutions lacking redox buffer (not regulated), and with oxidizing 4:1 GSH:GSSG or reducing 30:1 GSH:GSSG. *, a significant difference between the absence and presence of CLIC-2 in each condition. #, a significant difference between the control measurements in the redox regulated and redox unregulated situations.

Chamelion properties of CLIC-2

We have focused on the interaction between CLIC-2 and RyR2. However, the CLIC proteins have a broad tissue and cellular distribution and a broad range of functions (6, 7). CLIC proteins are found in mammals, birds, fish, and amphibia, as well as in sea squirts, nematodes, and insects. There are six human CLIC proteins, each having a conserved 230 residues core and a less conserved hydrophilic N-terminal part. The proteins are found in nuclear, lysosomal, Golgi, and plasma membrane, mitochondria, and cell–cell junctions, and are implicated in kidney function, cell division, and bone resorption (3, 17, 30, 31). CLIC Cl^- channels are linked to neurotoxicity in Alzheimer's disease, apoptosis in several cell types, and slowed tumor growth (6, 7). CLIC proteins are targets for phosphorylation and associate with cytoskeletal and scaffold proteins, as well as with RyR2 (3, 4, 12, 28).

The ability of CLIC-2 to transform from a water-soluble protein at pH 8 to a lipid embedded Cl^- channel at pH 5 is abolished by 5 m*M* DTT (7). The conversion of CLIC-2 from a RyR2-inhibitor to a RyR2-activator with a more reducing redox potential might involve structural changes in the protein that are related to the structural changes that determine its ability to form Cl^- channels. We assume that the soluble form of CLIC-2 interacted with RyR2 since the present experiments were performed at pH 7.4. We did not see any evidence of CLIC-2 induced Cl^- channels, both because the pH was unfavorable and because Cs methanesuphonate (the major anion) was used to block Cl^- channels.

The physiological significance of CLIC-2 modulation of RyR2

The physiological role of CLIC-2 is obscure since it does not possess glutathione *S*-transferase activity. Modulation of RyR2 activity is one of the few functional roles ascribed to the protein. The fact that CLIC-2 has the ability to decrease or increase RyR2 channel activity depending on redox potential indicates that it may regulate cytosolic Ca^{2+} in a manner that depends on the cellular environment. The result in Fig. 5 suggests that CLIC-2 may have little effect on RyR2 in healthy cells, but exerts a strong inhibitory effect when the redox potential in the cytoplasm is more oxidizing, as in cardiac ischemia. Oxidative stresses in ischemia lead to high cytosolic Ca^{2+} that is partly attributed to an increase in RyR2 activity (24). Since CLIC-2 inhibits RyR2 under these conditions, it may well play a role in limiting Ca^{2+} induced ischemic damage. This possibility warrants future investigation of CLIC-2 expression in cardiomyocytes in ischemic conditions or artificially controlled redox states.

The mechanism of redox potential- and CLIC-2 –induced modulation of RyR2 activity

It is established that extreme redox potentials lead to the formation or breakage of disulfides bonds involving cysteine residues. These effects cannot be reversed by washing out the redox reagents, but can be reversed by adding reducing or oxidizing reagents (13, 14, 22). The wash-out reversibility of effects of GSH:GSSG buffers suggest that disulfide bridges are not formed or broken. Instead, the redox-sensing ability of proteins is ascribed to electron redistribution through the CH2-SH of cysteine residues (16). Under oxidizing conditions, the sulfur atom would act as an electron-rich center (nucleophile), while under reducing conditions, the protonation of the sulfur would diminish this effect. Presumably the redox response of the RyR requires cysteine residues on the luminal parts of the RyR, exposed to the luminal solution, as well as other cysteine residues on its cytoplasmic domains exposed to the cytoplasmic solution. For the channel gating machinery to be redox sensitive, the electron distribution of CH2-SH groups of the luminal and cytoplasmic cysteines must be regulated by redox buffers. CLIC-2 is likely to alter RyR2 activity by binding directly to the RyR, rather than indirectly by binding to associated proteins, since purified CLIC-2 depresses purified RyR activity (11).

In summary, the data suggest a novel role of CLIC-2 as a redox-dependent regulator of RyR2 channel activity. CLIC-2 increases channel activity under reducing conditions, but decreases channel activity under more oxidizing conditions. We postulate a role for endogenous CLIC-2 in limiting ischemia-induced cellular damage in cardiac tissue.

Acknowledgments

We thank Suzy Pace and Joan Stivala for the preparation of cardiac SR vesicles, and Damian Triffett for the expression and purification of CLIC-2. The work was funded by National Health and Medical Research Council of Australia Grants #268027 and #471462.

Abbreviations

BAPTA, 1,2-bis-(o-aminophenoxy)-ethane-*N,N,N′,N′*-tetra-acetic acid; CLIC-2, chloride intracellular channel type 2; CsMS, cesium methane sulfonate; DMSO, dimethyl sulfoxide; DTT, dithiothreitol; EC coupling, excitation–contraction coupling; EST, expressed sequence tag; GSH, reduced glutathione; GSSG, oxidized glutathione; GST, glutathione transferase; GSTO1-1, glutathione transferase omega type 1-1; GSTM2-2, glutathione transferase mu type 2-2; I', mean open time; I'_F , fractional mean current ; I'_{max}, maximal mean current; PMSF, phenylmethylsulphonyl fluoride; OD, optical density; O_1, maximum current for a single channel; O_2, current level when 2 channels open simultaneously; P_o, open probability; RyR1, skeletal type ryanodine receptor; RyR2, cardiac type ryanodine receptor; SDS–PAGE, sodium dodecyl sulfate polyacrylamide gel electrophoresis; SEM, standard error of the mean; SR, sarcoplasmic reticulum; T_o, mean open time; T_c , mean closed time.

References

1. Abdellatif Y, Liu D, Gallant EM, Gage PW, Board PG, and Dulhunty AF. The Mu class glutathione transferase is abundant in striated muscle and is an isoform-specific regulator of ryanodine receptor calcium channels. *Cell Calcium* 41: 429–440, 2007.
2. Banhegyi G, Lusini L, Puskas F, Rossi R, Fulceri R, Braun L, Mile V, di Simplicio P, Mandl J, and Benedetti A. Preferential transport of glutathione versus glutathione disulfide in rat liver microsomal vesicles. *J Biol Chem* 274: 12213–12216, 1999.
3. Berryman MA and Goldenring JR. CLIC4 is enriched at cell–cell junctions and colocalizes with AKAP350 at the centrosome and midbody of cultured mammalian cells. *Cell Motil Cytoskeleton* 56: 159–172, 2003.
4. Board PG, Coggan M, Watson S, Gage PW, and Dulhunty AF. CLIC-2 modulates cardiac ryanodine receptor Ca^{2+} release channels. *Int J Biochem Cell Biol* 36: 1599–1612, 2004.
5. Chu A, Dixon MC, Saito A, Seiler S, and Fleischer S. Isolation of sarcoplasmic reticulum fractions referable to longitudinal tubules and junctional terminal cisternae from rabbit skeletal muscle. *Methods Enzymol* 157: 36–46, 1988.
6. Cromer BA, Morton CJ, Board PG, and Parker MW. From glutathione transferase to pore in a CLIC. *Eur Biophys J* 31: 356–364, 2002.
7. Cromer BA, Gorman MA, Hansen G, Adams JJ, Coggan M, Littler DR, Brown LJ, Mazzanti M, Breit SN, Curmi PM, Dulhunty AF, Board PG, and Parker MW. Structure of the Janus Protein Human CLIC2. *J Mol Biol* 374: 719–731, 2007.
8. Dulhunty A, Haarmann C, Green D, and Hart J. How many cysteine residues regulate ryanodine receptor channel activity? *Antioxid Redox Signal* 2: 27–34, 2000.
9. Dulhunty A, Gage P, Curtis S, Chelvanayagam G, and Board P. The glutathione transferase structural family includes a nuclear chloride channel and a ryanodine receptor calcium release channel modulator. *J Biol Chem* 276: 3319–3323, 2001.
10. Dulhunty AF, Cengia L, Young J, Pace SM, Harvey PJ, Lamb GD, Chan YN, Wimmer N, Toth I, and Casarotto MG. Functional implications of modifying RyR-activating peptides for membrane permeability. *Br J Pharmacol* 144: 743–754, 2005.
11. Dulhunty AF, Pouliquin P, Coggan M, Gage PW, and Board PG. A recently identified member of the glutathione transferase structural family modifies cardiac RyR2 substate activity, coupled gating and activation by Ca^{2+} and ATP. *Biochem J* 390: 333–343, 2005.
12. Duncan RR, Westwood PK, Boyd A, and Ashley RH. Rat brain p64H1, expression of a new member of the p64 chloride channel protein family in endoplasmic reticulum. *J Biol Chem* 272: 23880–23886, 1997.
13. Eager KR and Dulhunty AF. Activation of the cardiac ryanodine receptor by sulfhydryl oxidation is modified by Mg^{2+} and ATP. *J Membr Biol* 163: 9–18, 1998.
14. Eager KR and Dulhunty AF. Cardiac ryanodine receptor activity is altered by oxidizing reagents in either the luminal or cytoplasmic solution. *J Membr Biol* 167: 205–214, 1999.
15. Eu JP, Sun J, Xu L, Stamler JS, and Meissner G. The skeletal muscle calcium release channel: coupled O2 sensor and NO signaling functions. *Cell* 102: 499–509, 2000.
16. Feng W, Liu G, Allen PD, and Pessah IN. Transmembrane redox sensor of ryanodine receptor complex. *J Biol Chem* 275: 35902–35907, 2000.
17. Fernandez–Salas E, Sagar M, Cheng C, Yuspa SH, and Weinberg WC. p53 and tumor necrosis factor alpha regulate the expression of a mitochondrial chloride channel protein. *J Biol Chem* 274: 36488–36497, 1999.
18. Hain J, Onoue H, Mayrleitner M, Fleischer S, and Schindler H. Phosphorylation modulates the function of the calcium release channel of sarcoplasmic reticulum from cardiac muscle. *J Biol Chem* 270: 2074–2081, 1995.
19. Hidalgo C, Aracena P, Sanchez G, and Donoso P. Redox regulation of calcium release in skeletal and cardiac muscle. *Biol Res* 35: 183–193, 2002.
20. Laver DR, Roden LD, Ahern GP, Eager KR, Junankar PR, and Dulhunty AF. Cytoplasmic Ca^{2+} inhibits the ryanodine receptor from cardiac muscle. *J Membr Biol* 147: 7–22, 1995.
21. Leddy JJ, Murphy BJ, Qu Y, Doucet JP, Pratt C, and Tuana BS. A 60 kDa polypeptide of skeletal-muscle sarcoplasmic reticulum is a calmodulin-dependent protein kinase that associates with and phosphorylates several membrane proteins. *Biochem J* 295: 849–856, 1993.
22. Marengo JJ, Hidalgo C, and Bull R. Sulfhydryl oxidation modifies the calcium dependence of ryanodine-sensitive calcium channels of excitable cells. *Biophys J* 74: 1263–1277, 1998.
23. Meissner G. Ryanodine receptor/Ca^{2+} release channels and their regulation by endogenous effectors. *Ann Rev Physiol* 56: 485–508, 1994.
24. Menshikova EV and Salama G. Cardiac ischemia oxidizes regulatory thiols on ryanodine receptors: captopril acts as a reducing agent to improve Ca^{2+} uptake by ischemic sarcoplasmic reticulum. *J Cardiovasc Pharmacol* 36: 656–668, 2000.
25. Minum EW, King BM, and Bear G. *Statistical Reasoning in Psychology and Education,* Third Ed., New York, John Wiley & Sons, Inc, 1993.
26. Morad M, Suzuki YJ, and Okabe E. Redox regulation of cardiac and skeletal sarcoplasmic reticulum. *Antioxid Redox Signal* 2: 1–3, 2000.

27. Pessah IN, Kim KH, and Feng W. Redox sensing properties of the ryanodine receptor complex. *Front Biosci* 7: a72–79, 2002.
28. Suginta W, Karoulias N, Aitken A, and Ashley RH. Chloride intracellular channel protein CLIC4 (p64H1) binds directly to brain dynamin I in a complex containing actin, tubulin and 14-3-3 isoforms. *Biochem J* 359: 55–64, 2001.
29. Sun J, Xu L, Eu JP, Stamler JS, and Meissner G. Classes of thiols that influence the activity of the skeletal muscle calcium release channel. *J Biol Chem* 276: 15625–15630, 2001.
30. Tonini R, Ferroni A, Valenzuela SM, Warton K, Campbell TJ, Breit SN, and Mazzanti M. Functional characterization of the NCC27 nuclear protein in stable transfected CHO-K1 cells. *FASEB J* 14: 1171-1178, 2000.
31. Valenzuela SM, Martin DK, Por SB, Robbins JM, Warton K, Bootcov MR, Schofield PR, Campbell TJ, and Breit SN. Molecular cloning and expression of a chloride ion channel of cell nuclei. *J Biol Chem* 272: 12575–12582, 1997.
32. Whittington A, Vichai V, Webb G, Baker R, Pearson W, and Board P. Gene structure, expression and chromosomal localization of murine theta class glutathione transferase mGSTT1-1. *Biochem J* 337: 141–151, 1999.

Address reprint requests to:
Professor AF Dulhunty
Division of Molecular Bioscience
John Curtin School of Medical Research
Australian National University
PO Box 334, Canberra City
ACT 2601, Australia

E-mail: angela.dulhunty@anu.edu.au

Date of first submission to ARS Central, November 29, 2007; date of final revised submission, April 2, 2008; date of acceptance, April 3, 2008.

This article has been cited by:

1. K. Takano, D. Liu, P. Tarpey, E. Gallant, A. Lam, S. Witham, E. Alexov, A. Chaubey, R. E. Stevenson, C. E. Schwartz, P. G. Board, A. F. Dulhunty. 2012. An X-linked channelopathy with cardiomegaly due to a CLIC2 mutation enhancing ryanodine receptor channel activity. *Human Molecular Genetics* **21**:20, 4497-4507. [CrossRef]
2. Dan Liu, Ruwani Hewawasam, Yamuna Karunasekara, Marco G. Casarotto, Angela F. Dulhunty, Philip G. Board. 2012. The inhibitory glutathione transferase M2-2 binding site is located in divergent region 3 of the cardiac ryanodine receptor. *Biochemical Pharmacology* **83**:11, 1523-1529. [CrossRef]
3. P. Bhandari, J. S. Hill, S. P. Farris, B. Costin, I. Martin, C.-L. Chan, J. T. Alaimo, J. C. Bettinger, A. G. Davies, M. F. Miles, M. Grotewiel. 2012. Chloride intracellular channels modulate acute ethanol behaviors in Drosophila, Caenorhabditis elegans and mice. *Genes, Brain and Behavior* **11**:4, 387-397. [CrossRef]
4. K. S. Suh, M. Malik, A. Shukla, A. Ryscavage, L. Wright, K. Jividen, J. M. Crutchley, R. A. Dumont, E. Fernandez-Salas, J. D. Webster, R. M. Simpson, S. H. Yuspa. 2012. CLIC4 is a tumor suppressor for cutaneous squamous cell cancer. *Carcinogenesis* . [CrossRef]
5. Angela F. Dulhunty, Ruwani Hewawasam, Dan Liu, Marco G. Casarotto, Philip G. Board. 2011. Regulation of the cardiac muscle ryanodine receptor by glutathione transferases. *Drug Metabolism Reviews* **43**:2, 236-252. [CrossRef]
6. Daolin Tang , Rui Kang , Herbert J. Zeh III , Michael T. Lotze . 2011. High-Mobility Group Box 1, Oxidative Stress, and Disease. *Antioxidants & Redox Signaling* **14**:7, 1315-1335. [Abstract] [Full Text HTML] [Full Text PDF] [Full Text PDF with Links]
7. Robyn T. Rebbeck, Yamuna Karunasekara, Esther M. Gallant, Philip G. Board, Nicole A. Beard, Marco G. Casarotto, Angela F. Dulhunty. 2011. The #1a Subunit of the Skeletal DHPR Binds to Skeletal RyR1 and Activates the Channel via Its 35-Residue C-Terminal Tail. *Biophysical Journal* **100**:4, 922-930. [CrossRef]
8. Ruwani Hewawasam, Dan Liu, Marco G. Casarotto, Angela F. Dulhunty, Philip G. Board. 2010. The structure of the C-terminal helical bundle in glutathione transferase M2-2 determines its ability to inhibit the cardiac ryanodine receptor. *Biochemical Pharmacology* **80**:3, 381-388. [CrossRef]
9. John C. Edwards, Christina R. Kahl. 2010. Chloride channels of intracellular membranes. *FEBS Letters* **584**:10, 2102-2111. [CrossRef]
10. Isaac N. Pessah, Gennady Cherednichenko, Pamela J. Lein. 2010. Minding the calcium store: Ryanodine receptor activation as a convergent mechanism of PCB toxicity. *Pharmacology & Therapeutics* **125**:2, 260-285. [CrossRef]
11. Suresh K. JosephRole of Thiols in the Structure and Function of Inositol Trisphosphate Receptors **66**, 299-322. [CrossRef]